Available online at www.sciencedirect.com
SCIENCE DIRECT®
Journal of Photochemistry and Photobiology A: Chemistry 173 (2005) 1–6
Journal of Photochemistry and Photobiology A:Chemistry
www.elsevier.com/locate/jphotochem

Electrophoretically deposited TiO_2 photo-electrodes for use in flexible dye-sensitized solar cells

Jun-Ho Yum[a], Seok-Soon Kim[a], Dong-Yu Kim[a], Yung-Eun Sung[b,*]

[a] *Department of Materials Science and Engineering, Gwangju Institute of Science and Technology, Gwangju 500-712, Republic of Korea*
[b] *School of Chemical & Biological Engineering and Research Center for Energy Conversion and Storage, Seoul National University, Seoul 151-744, Republic of Korea*

Received 17 September 2004; received in revised form 25 November 2004; accepted 20 December 2004
Available online 21 January 2005

Abstract

The preparation of an electrophoretically deposited film composed of wide band gap nanocrystalline TiO_2 without the use of a surfactant or any post-thermal treatments is described. The resulting film was examined with reference to applications in a flexible dye-sensitized solar cell. The packing densities of the films could be controlled through electrophoretic deposition parameters, such as the applied electric field or the concentration of electrolyte. The fill factor and efficiency of energy conversion of the flexible dye-sensitized solar cell employing electrophoretically deposited TiO_2 film was 50% and 1.03%, respectively. To increase the efficiency of energy conversion of the flexible dye-sensitized solar cell, compression was employed and, as a result, the fill factor and efficiency of energy conversion increased to 56.3% and 1.66%, respectively. Thus, the fabrication of a flexible dye-sensitized cell by electrophoretic deposition without the need for any thermal treatment and surfactant is possible.
© 2004 Elsevier B.V. All rights reserved.

Keywords: Electrophoretic deposition; Flexible solar cell; Dye-sensitization; Packing density; TiO_2

1. Introduction

Nanocrystalline semiconducting films comprised of wide band-gap oxides are known to show extraordinary optical and electronic properties and are applicable for use in photovoltaics [1–3], photocatalysis [4], electrochromic [5–7], and batteries [8]. Nanocrystalline TiO_2 for use in photoelectrochemical cells based on dye-sensitized solar cells (DSCs) that were pioneered by O'Regan and Grätzel, have been the focus of numerous investigations during the last decade [1–3]. One of the current issues associated with DSCs is the fabrication of flexible DSCs, in which flexible transparent conductive substrates are used. The use of such substrates such as poly(ethylene terephthalate) coated with tin-doped indium oxide (ITO-PET) are known to have advantages in that they are not fragile, have a versatile shape, and their use is technologically advantageous. A porous network of nanocrystalline TiO_2 serves as the basis for many optoelecrical and electrical devices. Typically, a porous network of nanocrystalline TiO_2 in photovoltaic cells using glass can be readily prepared by sintering at 450–500 °C, a process that removes additives including organic surfactants [1–3]. However, this thermal treatment cannot be used in the preparation of a porous network of TiO_2 in flexible DSCs because of the susceptibility of the flexible substrates to degradation followed loosing their transparency and inducing distortion. Alternative routes, such as a thermal treatment at a temperature of around 130 °C [9–11] or compression [12,13] are employed for this purpose. Pichot et al. examined a surfactant-free coating of nanocrystalline TiO_2 with a thermal treatment of 100 °C and obtained a fill factor of 69% and an energy conversion efficiency of 1.2% [9]. De Paoli and coworkers demonstrated a flexible DSCs employing polymer electrolyte and obtained

* Corresponding author. Tel.: +82 2 880 1889; fax: +82 2 888 1604.
E-mail address: ysung@snu.ac.kr (Y.-E. Sung).

1010-6030/$ – see front matter © 2004 Elsevier B.V. All rights reserved.
doi:10.1016/j.jphotochem.2004.12.023

a fill factor of 42% and an energy conversion efficiency of 0.12% [11]. Hagfeldt and coworkers demonstrated a mechanically compressed nanostructured TiO_2 layer on a plastic film yielding a fill factor of 47% and a conversion efficiency of 3.0% [13]. In this study, the use of electrphoretic deposition (EPD) to produce a porous network of nanocrystalline TiO_2 for flexible DSCs was explored. EPD has been employed to produce photo-electrodes in DSCs [14,15]. Miyasaka et al. obtained a fill factor of 61% and a high conversion efficiency up to 4.1% with an electrophoretic TiO_2 layer following a chemical treatment and a thermal treatment of 150 °C for interconnecting TiO_2 particles [14]. In this study, the efficiency of DSCs were behind the Miyasaka el al. work, however, a packing density of TiO_2 layers could be controlled with small amount of water by using EPD and it is organic surfactant-free process without thermal treatment. A more detailed study of EPD for use in producing photo-electrodes is further necessary because EPD has certain advantages as mentioned below.

EPD represents a material processing technique in which charged particles in a suspension including an electrolyte, particles, additives and solvent are moved toward an oppositely charged electrode and are then deposited onto a substrate under an applied DC electric field. EPD is, therefore, a combination of electrophoresis and deposition. Applications of EPD for material processing are in widespread use in the fabrication of a variety of materials [16] including photoelectrodes in DSCs [14,15], phosphor screens [17–23], and ceramic coatings [24,25]. Some of the advantages of EPD include its low-cost, the fact that it is relatively fast and reproducible, and its potential for use in continuous processing. An organic surfactant-free process is another important advantage of EPD and the thickness, packing density or amount of colloids fabricated using EPD can be readily controlled by changing certain EPD parameters such as the electric field, concentration of electrolyte, and deposition time.

In this study, EPD parameters such as the zeta potential of particles and the packing density of the resulting film were examined and electrophoretically deposited nanocrystalline TiO_2 were used as photo-electrodes in flexible DSCs. We conclude, based on these findings, that electrophoretically deposited nanocrystalline TiO_2 has potential for use in flexible DSCs.

2. Experimental

ITO-PET (Toyobo, 60 Ω/□) was used as the substrate for the photo-electrodes and counter-electrode. The suspension for EPD used in the deposition was composed of nanocrystalline TiO_2 particles (P25, 20 nm, Degussa) in isopropyl alcohol (IPA, 99.5%, Junsei) containing 5×10^{-4} M $Mg(NO_3)_2{\cdot}6H_2O$ (Aldrich, 99.995 + %) including 2 vol.% deionized water (DI water). Stainless steel (SUS 304) was used as the anode during the EPD process and the distance between the anode and ITO-PET was fixed at 2 cm. Nanocrystalline TiO_2 powders were deposited on the ITO-PET using EPD under the following conditions; at various applied electric field and a suspension that contained 0.25 g/L of TiO_2.

The electrophoretic mobility of the suspended nanocrystalline TiO_2 was measured using an ELS-8000 (Otsuka Electronics, Japan). In this techniques, an electroosmosis flow under an electric field results in an electrophoretic flow. The electrophoretic mobility is then measured at different heights by light scattering. The measured electrophoretic mobility at the stationary layer is converted to the zeta potential.

For applying electrophoretically deposited nanocrystalline TiO_2 films to the photo-electrodes, a compression under 200 bar for 3 min was employed after the EPD process. The electrodes were immersed for 3 h in a 5×10^{-4} M solution of the sensitizer dye, Ru 535 (Solaronix) in pure ethanol. Pt sputtered ITO-PET was used as counter electrodes.

In the photochemical cell configuration, Ru 535/TiO_2 films on the ITO-PET were employed in a sandwich-type cell incorporating Pt sputtered ITO-PET and a non-aqueous electrolyte consisting of 0.5 M LiI, 0.05 M I_2, and 0.5 M *tert*-butylpyridine (TBP) in methoxypropionitrile. The cell was not sealed and was simply pressed and fixed by the clamps. The cell, whose active area is 0.16 cm^2, was tested under AM 1.5 solar conditions using a 500 W Xe lamp (Müller) and an AM 1.5 filter without IR and UV cut off filters. Photochemical behavior was investigated using a 1287A potentiostat/galvanostat (Solatron). The morphologies and thickness of the films were observed by SEM (S-4700, Hitachi) and an α-step profiler, respectively.

3. Results and discussion

The pH of an IPA containing $Mg(NO_3)_2{\cdot}6H_2O$ was approximately 4.7 and the nanocrystalline material used was similar to that used in our previous work [20]. The pH change of the solution by the addition of water was negligible. The value of the electrophoretic mobility of nanocrystalline TiO_2 in IPA was measured as a function of the concentration of $Mg(NO_3)_2{\cdot}6H_2O$. These electrophoretic mobility values were then converted to zeta potentials based on the Helmholtz–Smoluchowski equation (1) [26].

$$u = \varepsilon\xi/\eta \quad (1)$$

where u is the mobility of the particles, ε the product of ε_0 (vacuum permittivity) times ε_r (relative dielectric constant), ξ the zeta potential of the particles, and η the viscosity of the solvent.

The zeta potential is regarded as the potential at the outer Helmholtz plane (OHP)–diffuse layer interface in the Gouy–Chapman–Stern–Grahame model. The zeta potential of TiO_2 in pure IPA is approximately −22 mV. The zeta potential of the TiO_2 in the IPA changed as a function of the concentration of $Mg(NO_3)_2$ salt, as shown in Fig. 1. The zeta potential of TiO_2 in IPA in the presence of a low concentration of $Mg(NO_3)_2$ salt, 10^{-7} M, also had a negative

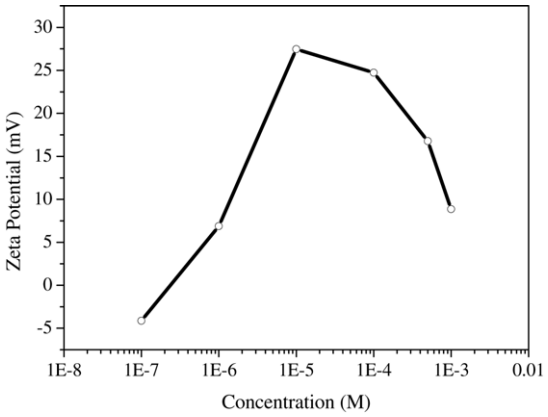

Fig. 1. Zeta potentials of TiO_2 particles as a function of concentration of $Mg(NO_3)_2$ salt in the IPA.

value of approximately −4.1 mV. The value was increased with increasing concentration of $Mg(NO_3)_2$ salt and reached a maximum of 27.5 mV at 10^{-5} M. The zeta potential was decreased to 8.9 mV at 10^{-3} M with an increase in the concentration of $Mg(NO_3)_2$ salt. This result is in agreement with previous published data [17]. The change in zeta potential from a negative to a positive value resulted from the increased negative charge density of the diffuse layer which compensates for the increase in $MgNO_3^+$ adsorbed to the particle surface. The decrease in zeta potential with a further increase in concentration resulted from an increased negative charge density in the diffuse layer while the sites available for ion adsorption were saturated [17]. The value of the zeta potential for nanocrystalline TiO_2 in suspension comprised of 5×10^{-4} M $Mg(NO_3)_2$ salt in IPA was found to be approximately 16.7 mV. This value increased to approximately 19.3 mV when water was added to the suspension, as has been described previously [20]. The addition of water is known to increase the adhesive strength of electrophoretically deposited particles [19,20]. In our work, water was also added to increase adhesive strength and to prevent nanocrystalline TiO_2 particles from being dislodged during processes such as measuring the photocurrent of the TiO_2 films. The water further may also affect the packing density of TiO_2 films, as discussed below. The zeta potential is known to be an important indicator of the rate of deposition of particles during EPD and the stability of the suspension against coagulation or settling [23]. A high zeta potential value may result in a high deposition rate and minimal coagulation. This is discussed below.

The particle packing density (packing ratio) is the ratio of the volume of the substantial parts (V_s) to the total volume of the packed powders (V) [27]. The packing density can be calculated using Eq. (2) [20,27]:

$$P = V_s/V = M/At\rho \quad (2)$$

where M is the total mass (mg), t the thickness of the TiO_2 film, A the deposited area, and ρ the density of the TiO_2 powder. The density of rutile and anatase TiO_2 is 4.26 and 3.89 g/cm^3, respectively [28]. The TiO_2 powder (P25) used in this work consisted of 70% anatase TiO_2 and 30% rutile TiO_2, and the density of the material was 4.00 g/cm^3. The packing density of a TiO_2 film fabricated using EPD is dependent on the applied voltage as shown in Fig. 2. Other deposition parameters, such as the deposition time, were fixed and only the electric field was changed. Open circles and closed squares indicate the current during the EPD and the packing density of TiO_2 films, respectively. The current was about 0.2 mA when the EPD was carried out at electric field under 10 V/cm and the packing density of the TiO_2 film was about 42% (shown as %). As the electric field was increased to 25, 50, and 75 V/cm, the applied current was proportionally increased to 1.6, 3.6, and 6 mA. This increase of current resulted in a decrease of the packing densities of the TiO_2 films, the values of which were about 38%, 34%, and 26% for a current of 1.6, 3.6, and 6 mA, respectively. The packing density was dependent on the current because of the hydrolysis of water present at the cathode. An increase in hydrolysis due to a high current under a high electric field might result in the evolution of hydrogen followed by interrupting particles deposition or leaving vacancies and would finally induce a low packing density in the films [19,20]. At a concentration of $Mg(NO_3)_2$ salt in the IPA of 10^{-3} M and an electric field of 75 V/cm, the packing density of the TiO_2 film, after EPD, was increased by approximately 30%, and the deposit was low in comparison with a film deposited under experimental conditions. This results from the low deposition rate due to a low zeta potential, which also affects the increase in packing density. TiO_2 particles must overcome repulsive barriers to induce coagulations, leading to the production of a dense mass during EPD [24]. The low repulsive barrier due to the low zeta potential of TiO_2 particles might induce a high packing density in a TiO_2 film. The packing density of the TiO_2 films could be easily controlled by appropriate alteration in the EPD.

In a photochemical cell configuration, the current density (J)–voltage (V) characteristics, for a cell comprised of

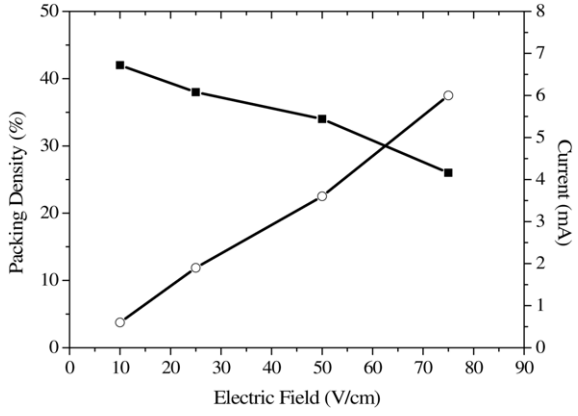

Fig. 2. Packing density of a TiO_2 film and current during the EPD as a function of electric field, (■) packing density of the TiO_2 film, (◯) current during the EPD.

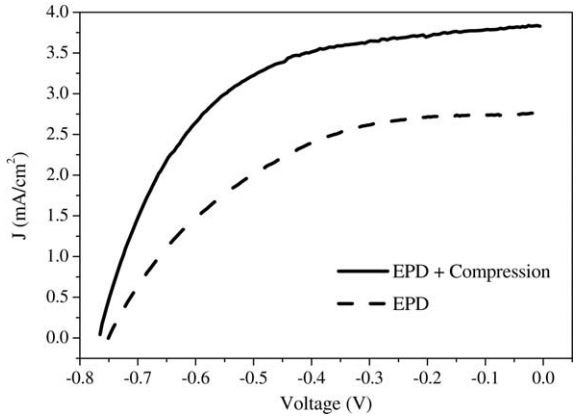

Fig. 3. Current density–voltage characteristics of TiO_2 films deposited using EPD (dashed line) and EPD combined with compression (solid line). The counter electrode is a Pt-coated ITO-PET. The electrolyte consists of 0.5 M LiI, 0.05 M I_2, and 0.5 M *tert*-butylpyridine (TBP) in methoxypropionitrile. The cell was tested under AM 1.5 solar condition.

a Ru(dye)/TiO_2 film fabricated by immersion in a Ru dye solution and EPD, a non-aqueous electrolyte containing an I_3^-/I^- redox, and a Pt-coated ITO-PET, was investigated under AM 1.5 solar conditions with no additional filters such as IR or UV cut offs, as shown in Fig. 3. TiO_2 films produced by EPD under the following conditions: 75 V/cm for 180 s in a 0.25 g/L TiO_2 suspension have a thickness of 8.5 μm. A dashed line indicates the *J–V* characteristic of the flexible DSCs under 1 sun. The open circuit voltage (V_{oc}) and short circuit current density (J_{sc}) of the flexible DSCs was found to be −0.751 V and 2.74 mA/cm^2 under 1 sun, respectively. The fill factor (ff) and efficiency of energy conversion (η) of the flexible DSCs was 50% and 1.03%, respectively. The fill factor (ff) and efficiency for energy conversion (η) were calculated from Eqs. (3) and (4):

$$\mathrm{ff} = I_m V_m / I_{sc} V_{oc} \quad (3)$$

$$\eta = I_{sc} V_{oc} \mathrm{ff} / I_s \quad (4)$$

where $I_m V_m$ is the maximum power and I_s the intensity of the incident light.

The low efficiency of DSCs may result from a relatively poor interconnection between the nanocrystalline TiO_2 compared to the film that had undergone a thermal treatment. The compression method [12,13] was used as a posttreatment in an attempt to increase the interconnection of TiO_2 in the flexible DSCs prepared by EPD. The morphologies of the films were clearly changed after the application of compression, evidenced by SEM images, for the TiO_2 films prepared using only EPD and EPD combined with compression as shown in Fig. 4. The SEM images of nanocrystalline TiO_2 films deposited by EPD are shown in Fig. 4(a) and (b). A mesoporous structure of nancrystalline TiO_2, with a pore size below about 80 nm and a large percentage of several tens of nanometers, could be obtained using EPD as investigating surface (Fig. 4(a)) and cross-sectional (Fig. 4(b)) SEM images. When a compression at 200 bar was applied for

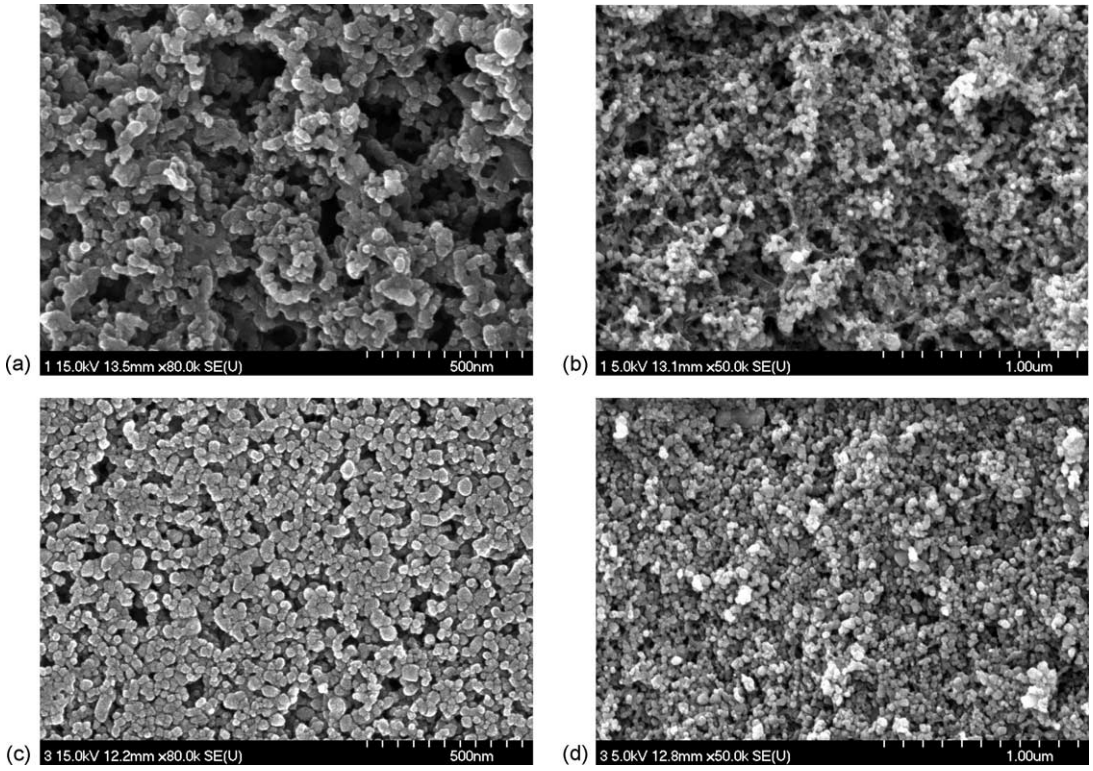

Fig. 4. SEM micrographs of electrophoretically deposited TiO_2 fabricated by EPD and EPD combined with compression on an ITO-PET, (a and b) EPD without compression and (c and d) with compression at 200 bar for 3 min, (b and d) cross-sectional view.

3 min to nanocrystalline TiO_2 films deposited using EPD, the thickness of the films decreased to about 4 μm without any change in the deposited weight. The pore size of the compressed nanocrystalline TiO_2 was below 10 nm except some of relatively large pores. Thus, after compression, the films exhibited more packed morphologies than films prepared by only EPD, as shown in Fig. 4(c) and (d). This result would be expected, based on the large decrease in film thickness, about 50%, after compression. The packing densities of the TiO_2 films to which compression had been applied after EPD show values of almost 60%. The application of compression to TiO_2 film deposited by EPD resulted in a more densely packed TiO_2 film and this result also was confirmed by inspection of surface (Fig. 4(c)) and cross-sectional (Fig. 4(d)) SEM images. Thus, an improvement in interconnection between nanocrystalline TiO_2 after compression would be expected and this would result in an increase in the efficiency of energy conversion of the flexible DSCs.

The *J–V* characteristics of a TiO_2 photo-electrode fabricated by EPD with a subsequent compression process are shown in Fig. 3. A solid line indicates the *J–V* characteristic of the flexible DSCs under 1 sun. The open circuit voltage and short circuit current density of the flexible DSCs that were subjected to compression was −0.765 V and 3.84 mA/cm^2 under 1 sun (100 mW/cm^2) intensity. The fill factor and efficiency of a cell (solid line) that had undergone compression after EPD increased to 56.3% and 1.66%, respectively, while the original cell (dashed line) without compression yielded an efficiency of 1.03%, as mentioned above. The current density and fill factor increased and this result is an evidence for the improvement in interconnection between nanocrystalline TiO_2 after compression. The open circuit voltage of these cells yielded a high value, and this might result from the high resistance of flexible films. However, more study will be required to completely understand this result.

4. Conclusions

Nanocrystalline TiO_2 could be deposited on conductive substrates such as ITO-PET by EPD. The zeta potential of TiO_2 particles in the IPA was dependent on the concentration of magnesium nitrate salt used and the packing density of the TiO_2 films and could be controlled by adjustment in the electric field and hanging the concentration of magnesium nitrate salt present. A high current under a high electric field might result in low packing density in the films. The low repulsive barrier due to the low zeta potential of TiO_2 particles might induce a high packing density in a TiO_2 film.

Mesoporous TiO_2 films deposited by EPD without or organic surfactants and post-thermal treatment were examined with reference to applications to photo-electrodes in flexible DSCs. The fill factor and efficiency of energy conversion of the flexible DSCs was 50% and 1.03%, respectively. A cell with a TiO_2 film that had undergone compression after EPD yielded a fill factor of 56.3% and an efficiency of 1.66%. This increase in fill factor and efficiency might result from improvements in interconnections between TiO_2 particles. Thus, it is possible to fabricate the flexible DSCs by EPD without the need for any organic surfactant or any thermal treatment.

Acknowledgments

This work was supported by the Sol–Gel Innovation Project (SOLIP) funded by the Ministry of Commerce, Industry and Energy, and KOSEF through the Research Center for Energy Conversion and Storage, and the Brain Korea 21 project from the Ministry of Education.

References

[1] B. O'Regan, M. Grätzel, Nature 353 (1991) 737–740.
[2] M.K. Nazeeruddin, A. Kay, I. Rodicio, R. Humphry-Backer, E. Mueller, P. Liska, N. Vlachopoulos, M. Grätzel, J. Am. Chem. Soc. 115 (1993) 6382–6390.
[3] C.J. Barbé, F. Arendse, P. Comte, M. Jirousek, F. Lenzmann, V. Shklover, M. Grätzel, J. Am. Ceram. Soc. 80 (1997) 3157–3171.
[4] K. Vinodaopal, S. Hotchandani, P.V. Kamat, J. Phys. Chem. 97 (1993) 9040–9044.
[5] X. Marguerettaz, R. O'Neill, D. Fitzmaurice, J. Am. Chem. Soc. 116 (1994) 2629–2630.
[6] A. Hagfeldt, N. Vlachopoulos, M. Grätzel, J. Electrochem. Soc. 141 (1994) L82–L84.
[7] D. Liu, P.V. Kamat, J. Electrochem. Soc. 142 (1995) 835–839.
[8] S.Y. Huang, L. Kavan, M. Gratzel, J. Electrochem. Soc. 142 (1995) L142–L143.
[9] F. Pichot, J.R. Pitts, B.A. Gregg, Langmuir 16 (2000) 5626–5630.
[10] M.-A. De Paoli, A.F. Nogueira, D.A. Machado, C. Longo, Electrochim. Acta 46 (2001) 4243–4249.
[11] C. Longo, A.F. Nogueira, H. Cachet, M.-A. De Paoli, J. Phys. Chem. B 106 (2002) 5925–5930.
[12] H. Lindström, A. Holmberg, E. Magnusson, S.-E. Lindquist, L. Malmqvist, A. Hagfeldt, Nano Lett. 1 (2001) 97–100.
[13] H. Lindström, A. Hormberg, E. Magnusson, L. Malmqvist, A. Hagfeldt, J. Photochem. Photobiol. A 145 (2001) 107–112.
[14] T. Miyasaka, Y. Kijitori, T.N. Murakami, M. Kimura, S. Uegusa, Chem. Lett. 12 (2002) 1250–1251.
[15] T. Miyasaka, Y. Kijitori, J. Electrochem. Soc. 151 (2004) A1767–A1773.
[16] O.O. Van der Biest, L.J. Vandeperre, Annu. Rev. Mater. Sci. 29 (1999) 327–352.
[17] M.J. Shane, J.B. Talbot, R.D. Schreiber, C.L. Ross, E. Sluzky, K.R. Hesse, J. Colloid Interf. Sci. 165 (1994) 325–333.
[18] Y.W. Jin, J.E. Jang, W.K. Jung, N.S. Lee, J.M. Kim, D.Y. Jeon, J.P. Hong, J. Vac. Sci. Technol. B 17 (1999) 489–493.
[19] B.E. Russ, J.B. Talbot, J. Electrochem. Soc. 145 (1998) 1245–1252.
[20] J.H. Yum, K.H. Choi, Y.E. Sung, J. Electrochem. Soc. 150 (2003) H43–H46.
[21] J.H. Yum, S.Y. Seo, S.H. Lee, Y.E. Sung, J. Electrochem. Soc. 150 (2003) H47–H52.
[22] J.H. Yum, Y.E. Sung, J. Electrochem. Soc. 151 (2004) H27–H32.
[23] M.J. Shane, J.B. Talbot, E. Sluzky, K.R. Hesse, Colloid Surf. A 96 (1995) 301–305.

[24] P. Sakar, P.S. Nicholson, J. Am. Ceram. Soc. 79 (1996) 1987–2002.
[25] B. Ferrari, R. Moreno, P. Sakar, P.S. Nicholson, J. Euro. Ceram. Soc. 20 (2000) 99–106.
[26] P.C. Hiemenz, R. Rajagopalan, Principles of Colloid and Surface Chemistry, 3rd ed., Marcel Dekker, New York, 1997.
[27] S. Shionoya, W.M. Yen, Phosphor Handbook, CRC Press, Boca Raton, 1999.
[28] K. Kalyanasundaram, M. Grätzel, Coord. Chem. Rev. 77 (1998) 347–414.